Progress Report and Beamline Performance

All of the beamline components have been installed and commissioned. Figure 1 shows the plan and elevation views of the beamline. The X-ray beams travels from the right to the left in this figure. There are three lead-lined structures that enclose the beamline. The first enclosure to the right houses a beam-defining mask for the synchrotron radiation and bremsstrahlung radiation collimators. Most of the beamline X-ray optics are housed in the second enclosures. The major optical components are a moveable fixed aperture mask (primary aperture), a white beam filter (F2-30), two double crystal monochromators, a vertical focusing mirror, monochromatic beam defining slits (collimator slits) and a monochromatic photon shutter. The entire X-ray beam path is under ultra-high vacuum until the beam exits the beamline in the experimental enclosure at the far left in the figure.

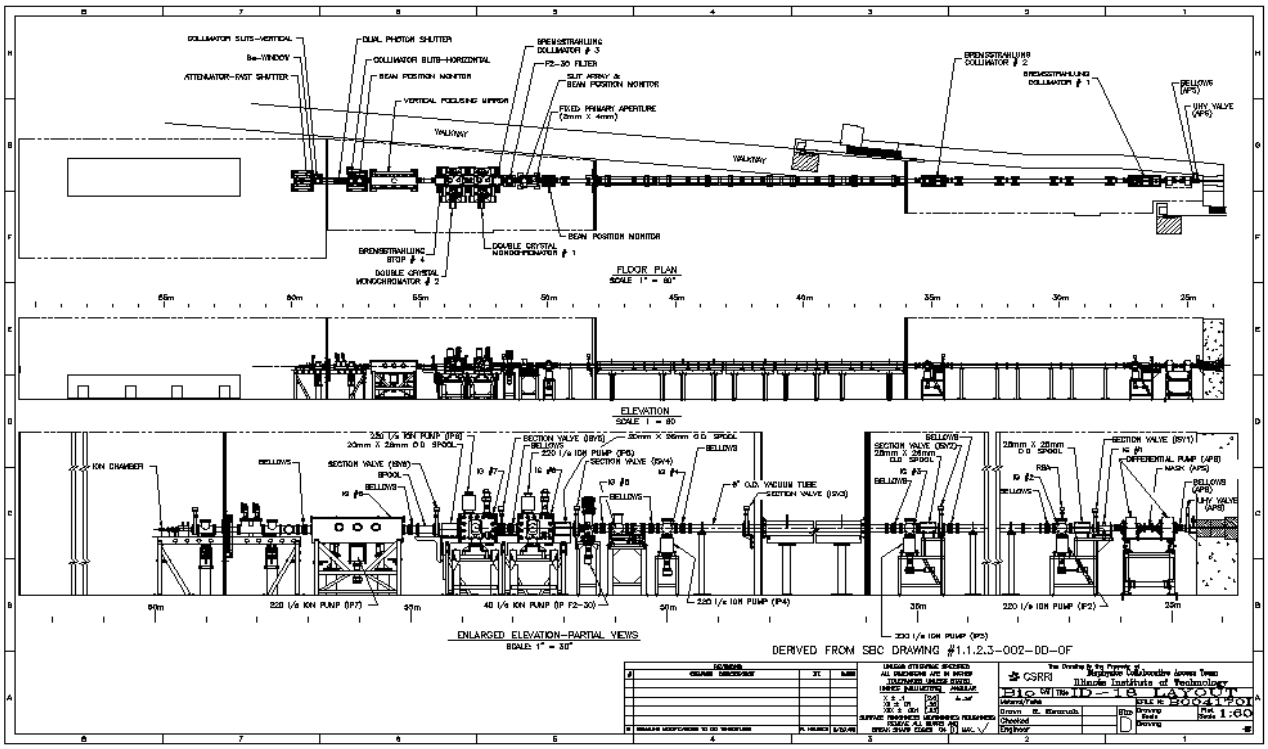

Figure 1. The plan and elevation views of the BioCAT beamline at sector 18 of the Advanced Photon Source at Argonne National Laboratory.

The moveable fixed mask has an aperture of 4.2 mm x 2.1 mm and serves two functions. The primary function is to reduce the heat load on the first monochromator crystal without significantly reducing the flux through the mask. The secondary function is to serve as a white beam position monitor.

The F2-30 has two arrays of filters that can be moved into the white X-ray beam in order to further reduce the power onto the first monochromator crystal. Currently, we are using graphite filters.

The monochromators are spectroscopy grade, constant exit height, double-crystal monochromators. The monochromators have identical mechanisms, but they are equipped with different crystals. Monochromator #1 has Si crystals with a (111) orientation, while those in monochromator # 2 have a (400) orientation. The user can select, under computer control, which monochromator they want to use based on the energy range or resolution that is desired. The energy range of monochromator #1 (Si(111)) is from 3.4 KeV to 14.6 KeV. Both monochromators were commissioned using water-cooled first crystals. This allowed us to bring the line up quickly (less than two years after the NIH support started). A new Si-cyro-cooled first crystal was designed as a collaborative effort between BioCAT, IMCA-CAT, MR-CAT and SBC-CAT. This was implemented in monochromator #1 in October of 1998 (Figure 2).

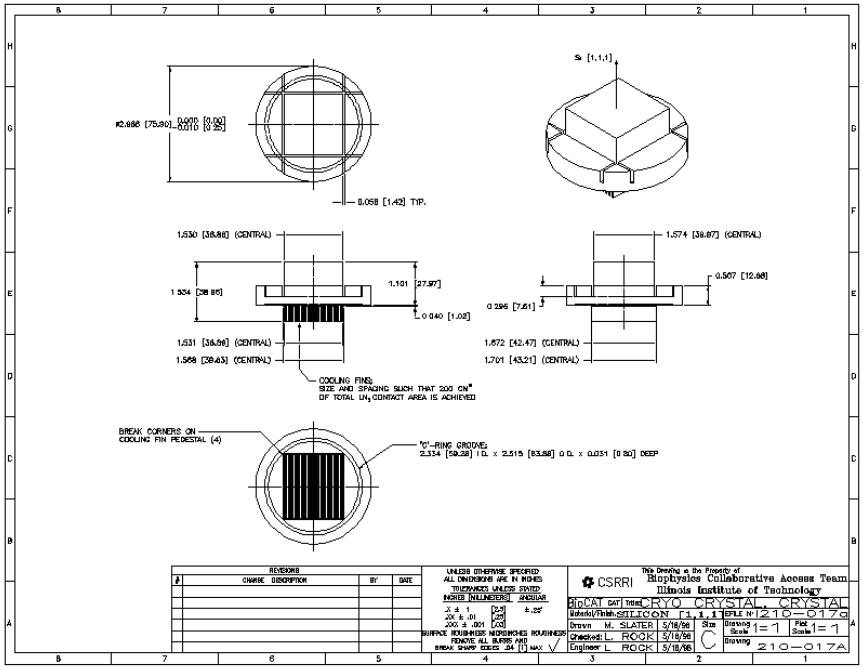

Figure 2. The new cryo-cooled monochromator crystal design.

It is interesting to note that the flux measured with the water cooled-crystal was approximately 20% higher than with the cryo-cooled crystal. However, the beam shape and rocking curve widths degraded quickly as the energy was decreased below 10 KeV. Table 1 lists the measured flux at select energies through the energy range of the Si(111) cryo-cooled monochromator. The APS requires the beamline vacuum-to-air exit window to be a double barrier. Thus the two 0.2 mm thick Be-exit windows account for most of the intensity fall off at lower energies. The size of the beam is approximately 1 mm x 5 mm (HxW) in the experimental enclosure.

Energy	Photons/sec/~0.1% BW/100 mA
12	1.78E+13
11	2.46E+13
10	2.51E+13
9	2.44e+13

8	2.14e+13
7	1.6.2e+13
6	1.00e+13
5	4.50e+12
4	3.10e+12

Table 1.

The X-ray source is an undulator insertion device. For a given magnetic pole gap, the undulator has a particular fundamental energy and higher harmonic energies. As the gap is decreased, the fundamental energy shifts towards lower energies and power output of the undulator rises quickly. The maximum X-ray flux is obtained by using the fundamental peak for energies less than 10 KeV, the third harmonic for energies in the range of 10 to 20 KeV, and the fifth harmonic for energies above 20 KeV. The effect of heat loading on the cryo-crystal was evaluated by recording the rocking curve of the double crystal monochromator at 12.0 KeV when the undulator energy was set for a fundamental energy of 12.0 KeV. When the undulator is set for a fundamental energy of 12.0 KeV the power absorbed by the first crystal is a modest 50 W per 100 mA of beam current. Figure 3 shows that the experimentally determined rocking curve (FWHM = 31.1 microradians) agrees quite well with the theoretical curve (FWHM = 31.7 microradians) under these conditions. However, when the undulator is set for a fundamental energy of 4.0 KeV the power absorbed in the first crystal is 375 W per 100 mA of beam current. It can be seen in Figure 3 that the increased power has caused the rocking curve of the third harmonic at 12.0 KeV to increase in width by about 24%. Other measurements at 6.0 KeV have show that by increasing the liquid nitrogen flow rate that the rocking curve width can be reduced to the natural width. Both monochromators can accept the cryo-cooled first crystal assembly. A Si(400) cryo-cooled crystal of similar design will be installed in the second monochromator this summer.

An alarm system has been built for the cryo-pumping system. This will trigger from either a high pressure, a low pressure or insufficient liquid nitrogen in the subcooler. We plan to fully integrate the cryo-system into the beamline equipment protection system in the next four months. Currently, we have to exchange and refill liquid nitrogen supply dewars at intervals of 18 to 36 hours depending on the undulator power. The APS is installing a vacuum jacketed liquid nitrogen distribution system that is expected to be operation in the fall of 1999. BioCAT is responsible for the remaining 15 meters of vacuum jacketed transfer line to connect the distribution line to the cryo-system.

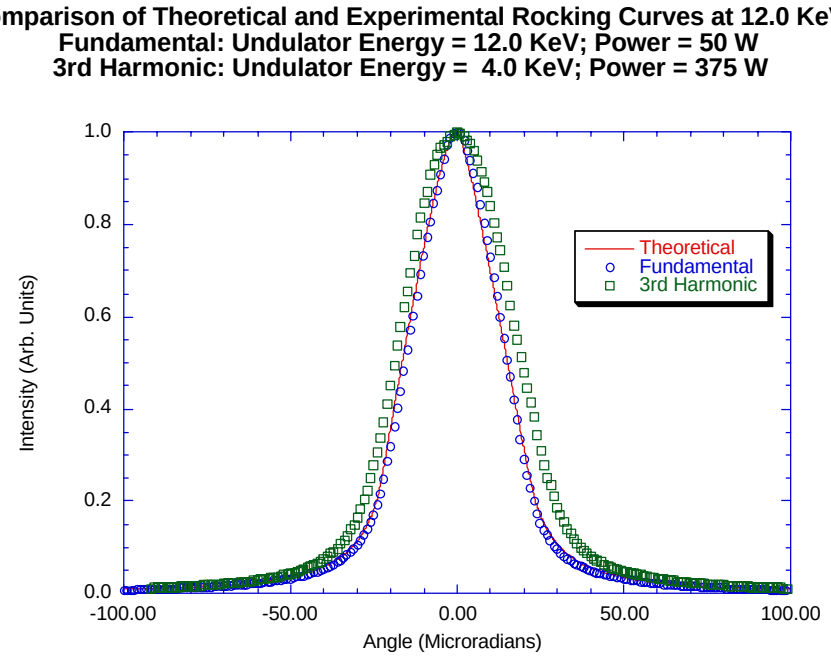

Figure 3. Comparison of the theoretical and experimentally determined rocking curves for the cryo-cooled Si(111) monochromator.

The second monochromator has an energy range of 7.9 KeV to 33.8 KeV with Si(400) crystals. This range can be extended up to 67.6 KeV by using the monochromator second harmonic reflection, namely Si(800). Intensity measurements with the water-cooled Si (400) crystal have show a flux of 1e12 photons/sec/100 mA at 25 KeV.

Both monochromators have sagittal focusing second crystal assemblies that can provide horizontal focusing of the beam. The horizontal width of X-ray beam is much narrower on an undulator beamline than on a bending magnet line. This allows one to design a sagittal focusing crystal that does not require stiffening ribs to minimize the effect of anticlastic bending. The result is that there is no loss of intensity when the beam is focused horizontally. Figure 4 shows the horizontal intensity profile of the 12.0 KeV sagittally focused beam at the focal point. This was measured at the focus of a 2 meter camera which corresponds to a demagnification ratio of 4.4:1. The focused beam has a FWHM = 169 micrometers. The maximum demagnification ratio is 6.2:1 and 7.3:1 for monochromator #1 and monochromator #2, respectively. The smallest horizontal beam focal width measured has a FWHM = 115 micrometers for the highest demagnification ratio.

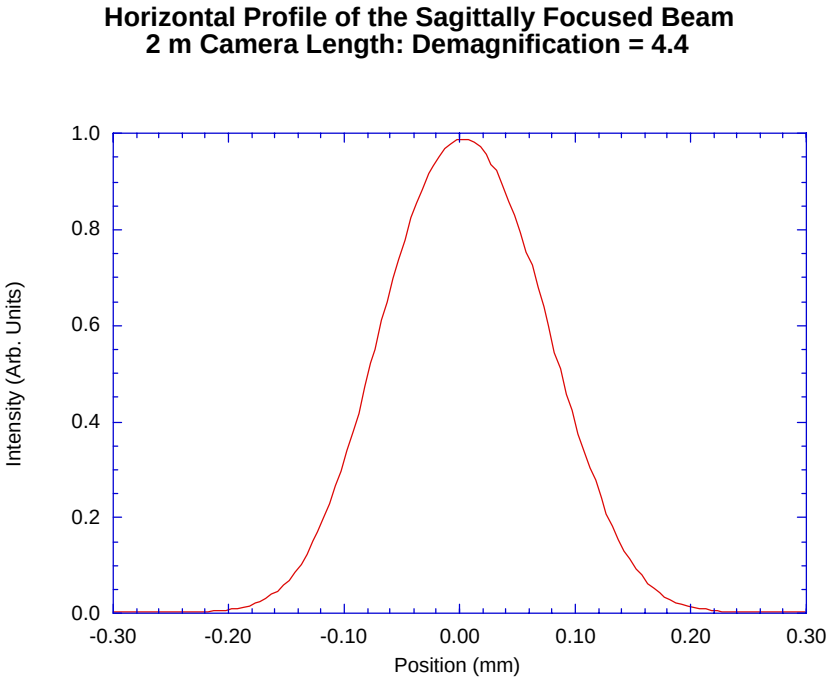

Figure 4. Horizontal Intensity Distribution of the Sagittally Focused Beam

The crystals of the double crystal monochromator are arranged in a nondispersive orientation. Thus the exit height of the beam was constant to 0.1 mm over the full energy range of the monochromator. However, the large temperature difference between the cryo-cooled first crystal and room temperature second crystal makes the double crystal monochromator slightly dispersive. Thus the monochromatic X-ray beam makes a slight angle relative to horizontal that is energy dependent. This means that the beam height at a given location will be a function of energy. The long lever arm between the monochromator and the specimen leads to height change on the order 80 micrometers/KeV at 4.0 KeV to 600 micrometers/KeV at 12 KeV. Fortunately, one can use the relative angle between the first and second crystals to steer the beam angle with an intensity loss of only a few percent in order to restore the constant exit height at a particular location. We have implemented an in-vacuum beam position monitor (BPM) that was developed by the SBC-CAT. This BPM is linear over a range of a few millimeters, and it has a resolution of less that 2 micrometers. Using this BPM and a feed-forward approach to adjust the beam angle, we have been able to maintain constant exit height to ±25 micrometers over an XAS scan. We are preparing to use the BPM with piezo electric positioners in a real time feedback loop to adjust the beam angle in order to maintain the exit height constant to ±10 micrometers or less.

The beamline mirror is used for harmonic rejection and vertical focusing. The mirror material is ULE and has dimensions of 1020 mm x 95 mm x 39 mm (LxWxH). The mirror was installed in the mirror bender and the assembly was taking to the metrology laboratory at the APS for inspection. The shape of the mirror was adjusted to compensate for the gravitation sag under its

own weight. The resulting figure had a RMS slope-error or 4 microradians over the central 800 mm of the 1020 mm long mirror. The RMS surface roughness was 1 – 2 A. The mirror surface is divided into three lanes: bare ULE, Pd coated, and Pt coated. The product of the energy and critical angle for the three surfaces are as follows, 30.51, 62.21 and 81.31 KeV*microradians for bare ULE, Pd coated, and Pt coated, respectively. Thus the mirror can be used for harmonic rejection over the full energy range of the beamline. The mirror reflectivity is greater than 97% at the energies measured to date.

The location of the mirror relative to the source point results in large demagnification of the source. Figure 5 shows the vertical intensity profile of a 12.0 KeV beam at the focal point. This was measured at the focus of a 1 meter camera which corresponds to a demagnification ratio of 7.6:1. The beam which was also focused at the same location in the horizontal direction had a measured FWHM = 30 micrometers. The true width is slightly smaller since a 10 micrometer slit was used to profile the intensity distribution. The beam profile has also been recorded at a demagnification ratio of 11.2:1 which resulted in a measured FWHM = 20 micrometers.
Figure 5. The vertical intensity distribution of the point focused beam at a demagnification ratio of 7.6:1.

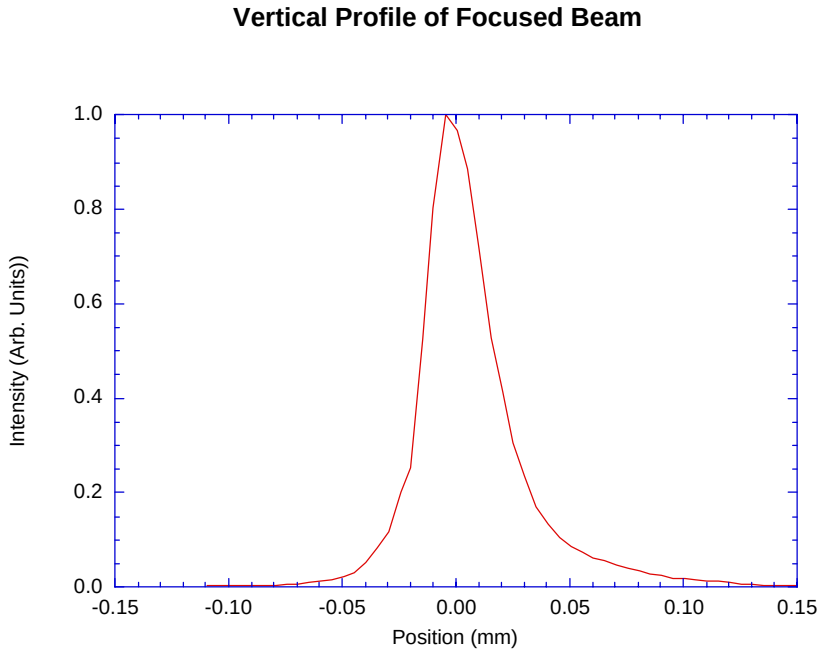

The focal point of the monochromator and mirror can be controlled independently. This allows one to optimize the beam shape separately in the horizontal and vertical directions at different locations. Thus one can optimize the intercept of the sample and the beam in one direction while still maintaining a sharp focus at the detector in the orthogonal direction, for example.

The beamline also has horizontal and vertical beam defining slits for the monochromatic beam after the mirror. These can be set to pass the entire beam or define a beam as small as 25 micrometers square.

The beam line also has a monochromatic photon shutter. This allows the X-rays optics to stay warm while allowing the user to entire the experimental enclosure.

The beamline was brought on line with the APS commissioning window separating the storage ring vacuum from the beamline vacuum. This significantly reduced the flux at lower energies. For example, at 4.0 KeV only about 3% of the X-ray beam was transmitted. We also had observed spatial modulations of intensity distribution of up to 50% in both the vertical and horizontal directions on length scales of 100 micrometers in the unfocused beam. This structure had been attributed to speckle diffraction arising form the interaction of the approximately 10% coherence of the undulator beam and the structure of the commissioning window. In August of 1997 the APS removed the commissioning window and installed a differential pump. This removed all windows between the beamline and the storage ring. Much to our surprise most of the structure still remained in the beam. Recently, we CITON polished the active surface of the cryo-crystal. Profiles of the unfocused beam using a 10 micrometer pinhole have shown that the structure in the beam is now gone.

The extremely high flux and excellent focal properties of the beamline meant that spectacular X-ray diffraction patterns could be recorded almost immediately when the beamline came on line. Similarly, we were able to record transmission XAS on metal foils immediately. However, XAS on dilute specimens has been a struggle. Much of our effort over the past year has been focused on improving the stability of the monochromator and linearity of response of the X-ray detectors. Recently, we recorded XAS form 0.5 mM Cu-Carbonate using a Lytle fluorescence X-ray detector with a filter and soller slits to reduce the intensity of elastically scattered X-rays. Figure 6 shows the results of a single scan recorded in step mode with a data collection time of 1 second/point. Although, the beam intensity had to be attenuated by a factor of 15 due to a nonlinearity between the incidence flux monitor and the Lytle detector, the signal to noise is quite good for a single scan. These data have identified two problems which we are currently working on.

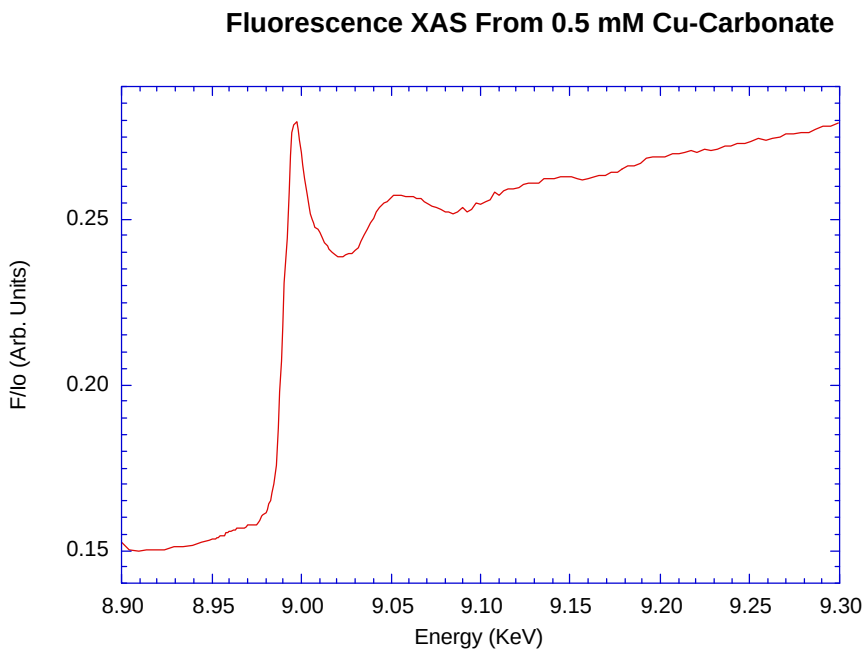

Figure 6. Single Fluorescence XAS Scan from a 0.5 mM Cu-Carbonate Solution. This was recorded in a step scan mode with 1 second data collection per point.

The multilayer analyzer detector was designed to handle the full available flux of an undulator beamline to record XAS from dilute specimens. However, in order to take full advantage of the detectors ability to reject the elastically scattered X-rays it requires the X-ray beam to be focused to 100 micrometers or less and to be stable to ±10 micrometers. As previously mentioned, this is being addressed with the piezo electric positioners and real time feedback of the beam position.

Even with the 15-fold attenuated intensity successive scans collected in step mode show deterioration of the specimen. Focusing the full beam intensity on 0.1 mm x 0.1 mm spot clearly requires that the spectra be recorded quickly. One way to record data quickly is to scan the monochromator energy continuously with an encoded DC-servo motor and to record data on the fly. The current approach allows us to record a 1000 eV XAS scans in 80 seconds with approximately 2 eV resolution. Figure 7 shows a continuous XAS scan of Au-foil recorded in transmission mode. The scan was recorded over a range of 500 eV in 80 seconds at a resolution of approximately 1 eV.

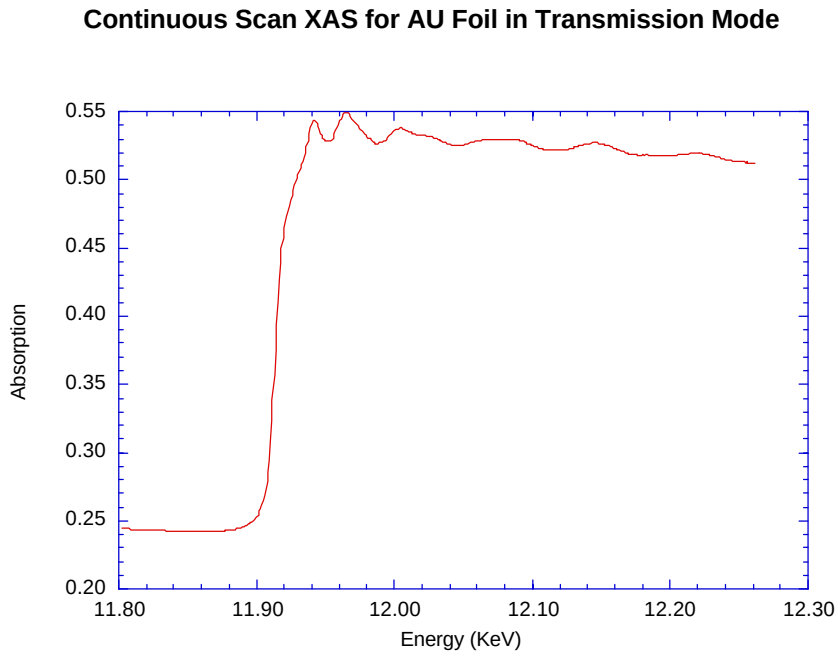

Figure 7. A Continuous XAS Scan of an Au-Foil Recorded in 80 seconds.

In the next few months will investigate recording continuous scans of dilute specimens. The current approach to continuous scans is limited to reading data at 100 millisecond intervals. We plan to move towards more rapid scans in two steps. The first step will use a rapid time-slicing scaler to record both the output of the X-ray detectors and the DC-servo motor encoder up/down pulses. The second step will be to program the PMAC intelligent motor controller to latch the scaler at predetermined energy intervals. This will allow full control of all the monochromator axes.